Functional characterization of the Mycobacterium tuberculosis zinc metallopeptidase Zmp1 and identification of potential substrates

Petrera, Agnese ; Amstutz, Beat ; Gioia, Magda ; Hähnlein, Janine ; Baici, Antonio ; Selchow, Petra ; Ferraris, Davide M ; Rizzi, Menico ; Sbardella, Diego ; Marini, Stefano ; Coletta, Massimo ; Sander, Peter

Functional characterization of the *Mycobacterium tuberculosis* zinc metallopeptidase Zmp1 and identification of potential substrates

Agnese Petrera[1,a], Beat Amstutz[1,a], Magda Gioia[2,3,a], Janine Hähnlein[1], Antonio Baici[4], Petra Selchow[1], Davide M. Ferraris[5], Menico Rizzi[5], Diego Sbardella[2,3], Stefano Marini[2,3], Massimo Coletta[2,3,*] and Peter Sander[1,6,*]

[1] Institute of Medical Microbiology, University of Zurich, Gloriastrasse 30/32, 8006 Zurich, Switzerland
[2] Department of Clinical Sciences and Translational Medicine, University of Roma Tor Vergata, Via Montpellier 1, I-00133 Roma, Italy
[3] Interuniversity Consortium for Research on Chemistry of Metals in Biological Systems, Via C. Ulpiani 27, I-70121 Bari, Italy
[4] Department of Biochemistry, University of Zurich, Winterthurerstrasse 190, 8057 Zurich, Switzerland
[5] Department of Chemical, Food, Pharmaceutical and Pharmacological Sciences, University of Piemonte Orientale "Amedeo Avogadro", Largo Donegani 2, I-28100 Novara, Italy
[6] Nationales Zentrum für Mykobakterien, Gloriastrasse 30/32, 8006 Zurich, Switzerland

*Corresponding authors
e-mail: coletta@seneca.uniroma2.it; psander@imm.uzh.ch

Abstract

Zinc metallopeptidases of bacterial pathogens are widely distributed virulence factors and represent promising pharmacological targets. In this work, we have characterized Zmp1, a zinc metallopeptidase identified as a virulence factor of *Mycobacterium tuberculosis* and belonging to the neprilysin (NEP; M13) family, whose X-ray structure has been recently solved. Interestingly, this enzyme shows an optimum activity toward a fluorogenic substrate at moderately acidic pH values (i.e., 6.3), which corresponds to those reported for the Mtb phagosome where this enzyme should exert its pathological activity. Substrate specificity of Zmp1 was investigated by screening a peptide library. Several sequences derived from biologically relevant proteins were identified as possible substrates, including the neuropeptides bradykinin, neurotensin, and neuropeptide FF. Further, subsequences of other small bioactive peptides were found among most frequently cleaved sites, e.g., apelin-13 and substance P. We determined the specific cleavage site within neuropeptides by mass spectrometry, observing that hydrophobic amino acids, mainly phenylalanine and isoleucine, are overrepresented at position P1′. In addition, the enzymatic mechanism of Zmp1 toward these neuropeptides has been characterized, displaying some differences with respect to the synthetic fluorogenic substrate and indicating that the enzyme adapts its enzymatic action to different substrates.

Keywords: drug development; enzyme kinetics; metallo-peptidase; *Mycobacterium tuberculosis*; peptide hormones; phagosome maturation.

Introduction

Tuberculosis (TB), the major bacterial cause of mortality around the world, kills about 2 million people annually, and approximately one third of the world's population is asymptomatically infected with *Mycobacterium tuberculosis* (Mtb), the main causative agent of the disease (WHO Fact sheet; http://www.who.int/mediacentre/factsheets/fs104/en/index.html). The prolonged coevolution of Mtb with its human hosts, and specifically with macrophages, has turned out in a peculiar survival strategy. Unlike other bacteria, which have developed different strategies, pathogenic Mtb has evolved to block lysosomal delivery (Nguyen and Pieters, 2005; Warner and Mizrahi, 2007). Hence, the pathogenic Mtb strategy demands that it actively subverts normal cellular mechanisms to avoid being killed (Nguyen and Pieters, 2005; Masjedi et al., 2006).

The Rv0198c gene of Mtb encodes for the zinc metallopeptidase 1 (Zmp1; 663 aa), which, although not required for mycobacterial growth *per se*, turned out to be essential for survival inside host macrophages (Master et al., 2008). An equivalent peptidase gene is also conserved in *Mycobacterium leprae* (MLCL622.12c; 667 aa), the causative agent of leprosy, whose genome exhibits massive gene decay (Cole et al., 2001). Master et al. (2008) have described Zmp1 as a secreted virulence factor of Mtb, involved in phagosome maturation arrest. Zmp1 manipulates host immune defence by interfering with the activation of a multiprotein complex termed inflammasome. Furthermore, *Zmp1* deletion influences the presentation of mycobacterial antigens, thus increasing the immunogenicity of vaccine strain *Mycobacterium bovis* Bacille Calmette-Guerin (Johansen et al., 2011). The important role of Zmp1 in Mtb pathogenicity has been recently confirmed in a mouse model (Muttucumaru et al., 2011), although some questioning about the mechanism remains open.

Zmp1 belongs phylogenetically to the MEROPS peptidase family M13 and displays the conserved HExxH active site

---

[a]These authors contributed equally to this work.

motif common to all Zn^{2+} metallopeptidases. The targets of M13 members usually are bioactive peptides with a key function in the regulation of cardiovascular, nervous, and immune systems (Turner et al., 2001). Zmp1 shares particularly primary sequence similarity (48%) with human neprilysin (NEP; 749 aa), an extracellular peptidase that preferentially hydrolyzes extracellular oligopeptides (<5 kDa) on the amino side of hydrophobic residues (also including amyloid β peptides implicated in Alzheimer disease) (Carson and Turner, 2002; Madani et al., 2006). We recently solved the crystal structure of Zmp1, and our investigation demonstrated that Zmp1 and NEP are also structurally conserved (Ferraris et al., 2011). A major aspect concerns the active site of Zmp1, which is accessible only through a narrow channel, rendering difficult the interaction with large macromolecular substrates; therefore, the enzyme seems more tailored to process peptides. Here we report the characterization of the proteolytic activity of Zmp1 metallopeptidase, describing its substrate preferences using a microarray-based peptide library and analyzing its cleavage specificity by mass spectrometry (MS). In addition, we have investigated the pH effect on Zmp1 catalysis, revealing an optimum activity at moderately acidic pH values, which are substrate-dependent.

Results

Zmp1 activity depends on Zn^{2+} binding

Mtb *Zmp1* was cloned into a prokaryotic expression vector carrying a His$_6$ modification at its N-terminus and heme agglutinin (HA) tag at its C-terminus for purification and detection. In addition, glutathione-*S*-transferase (GST)-*Zmp1*-His/HA tagged protein was cloned. Both proteins were expressed to high levels in *Escherichia coli* and purified in a two-step approach using HisTrap column and ion exchange/GST-sepharose beads. Purity was >95% according to a single band at the expected molecular weight in the SDS-PAGE (Figure 1A). Two mutants in the HExxH signature motif were produced by site-directed mutagenesis, namely H493A (His[493] was altered to Ala) and E494A mutant (Glu[494] was altered to Ala). Both mutated proteins were produced in a stable and soluble form and were purified to a high degree (Figure 1A and B).

To complement the crystallography data with the study of the protein in solution, circular dichroism (CD) spectroscopy was applied to Zmp1. In accord with the crystal structure (Ferraris et al., 2011), all purified forms of Zmp1 [i.e., wild type (wt) and the mutant] are properly folded, displaying identical CD spectra (Figure 1C). As predicted from the primary amino acid sequence and in agreement with the crystal structure (Ferraris et al., 2011), the secondary structure of Zmp1 displays over 70% of an α-helix structure, as estimated from the molar ellipticity at 222 nm (Morrow et al., 2000). Salts, such as $CaCl_2$ and NaCl, do not alter the thermal stability of Zmp1 helical folding (data not shown).

Zmp1 is able to cleave a synthetic fluorogenic substrate (see Materials and methods), which is specific for a family of zinc endoproteinases, called matrix metalloproteinases
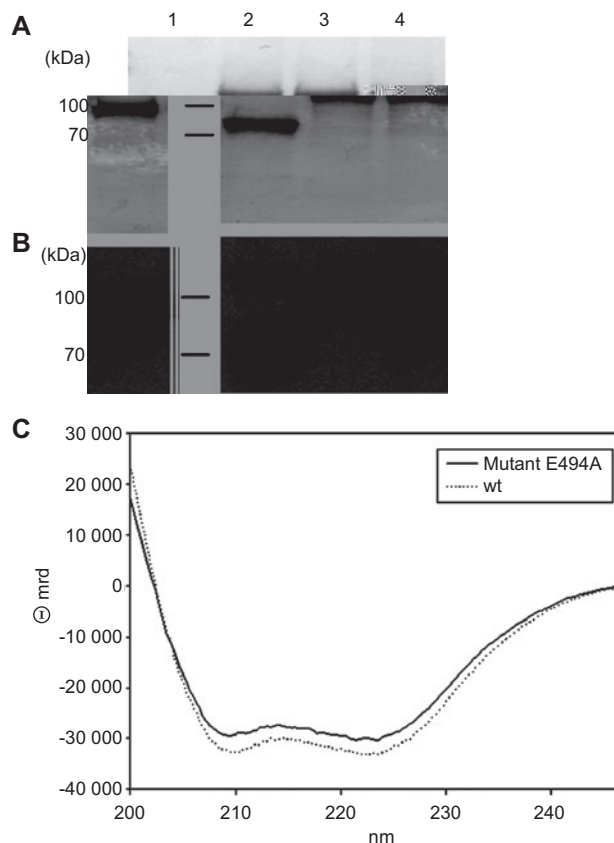

Figure 1 Purification of Zmp1 and its structure in solution.
(A) Coomassie stain of 12.5% SDS-gel and (B) Western blotting of Zmp1 variants. Lanes: 1, Zmp1 wt; 2, GST-Zmp1; 3, GST-Zmp1 E494A; 4, GST-Zmp1 H493A. Zmp1 shows the predicted molecular mass of 72 kDa. The three GST-tagged variants have a molecular mass of approximately 100 kDa due to the fusion with a 26-kDa GST tag. (C) CD spectra of Zmp1. Dashed line corresponds to the CD spectrum of the Zmp1 wt; continuous line refers to the inactive E494A Zmp1.

(MMPs), sharing the catalytic motif (i.e., HExxH) with the M13 family. GST-Zmp1 wt cleaved the fluorogenic substrate with high efficiency and, as expected, mutating the catalytic motif almost abolished the proteolytic activity. Likewise, EDTA and the Zn^{2+} chelator 1,10-phenanthroline reduced Zmp1 activity (see Table 1). Zmp1 activity was also strongly inhibited by the potent M13 metallopeptidase inhibitor phosphoramidon with a $K_I = 3.5(\pm0.5)\times10^{-8}$ M (Ferraris et al., 2011). The enzyme does not undergo autoproteolysis during

Table 1 Effect of peptidase inhibitors on the activity of Zmp1.

Inhibitor	Concentration (mM)	Zmp1 activity (% of control)
Phosphoramidon	0.1	5.1±1.2
1,10-Phenanthroline	0.1	7.8±3.2
EDTA	1	46.4±8.3

Zmp1 (10 nM) was preincubated with inhibitor for 10 or 60 min (in case of EDTA) at room temperature. Activity toward the synthetic fluorogenic substrate was measured after 5 min at 37°C (±SD).

the activity assay, as proven by the Selwyn test (Selwyn, 1965) (see Figure S1).

pH dependence of Zmp1 proteolytic activity

The pH dependence of Zmp1 activity was first measured using a synthetic fluorogenic substrate. From the analysis of the dependence on the substrate concentration at each pH value according to Eqs. (2) and (3) (see Materials and methods), we have obtained the catalytic parameters (i.e., k_{cat}/K_m, k_{cat}, and K_m) at each investigated pH. Their pH dependence is reported in Figure 2A–C for k_{cat}/K_m (A), k_{cat} (B), and K_m (panel C). obtaining the pK_a values reported in Table 2. Although the nonlinear least squares fitting of the pH dependence of individual parameters might have been carried out with only two protonatable groups, the global fitting of the pH dependence of all three catalytic parameters demanded three protonatable groups [i.e., n=3 in Eqs. (4a)–(4c); see Materials and methods]. Evidently, the overall enzymatic activity of Zmp1 (corresponding to k_{cat}/K_m) is highest at pH 6.3 (Figure 2A),

a pH value quite low compared with other metallopeptidases (Fasciglione et al., 2000). Further, the pH dependence of K_m (Figure 2C) indeed suggests that the substrate affinity tends to increase at pH lower than 7.5, as K_m decreases. An interesting pattern is observed for the pH dependence of k_{cat} (Figure 2B), where it appears evident that at least two groups with markedly different pK_a values are modulating this parameter. In particular, it is worth underlining that the two-protonated species appears to be the most active form of Zmp1 and that this enhanced activity is connected to a residue characterized by a pK_a=6.73±0.17 in the free enzyme, which then shifts to pK_a=7.72±0.16 in the substrate-bound form (Table 2). As a consequence, the pH-dependent profile of k_{cat} appears somewhat displaced toward higher pH values.

Zmp1 inhibition by Ilomastat

The inhibition constant by Ilomastat has been determined for Zmp1, exploiting the inhibitor concentration dependence of the substrate affinity (Figure 2D). Application of
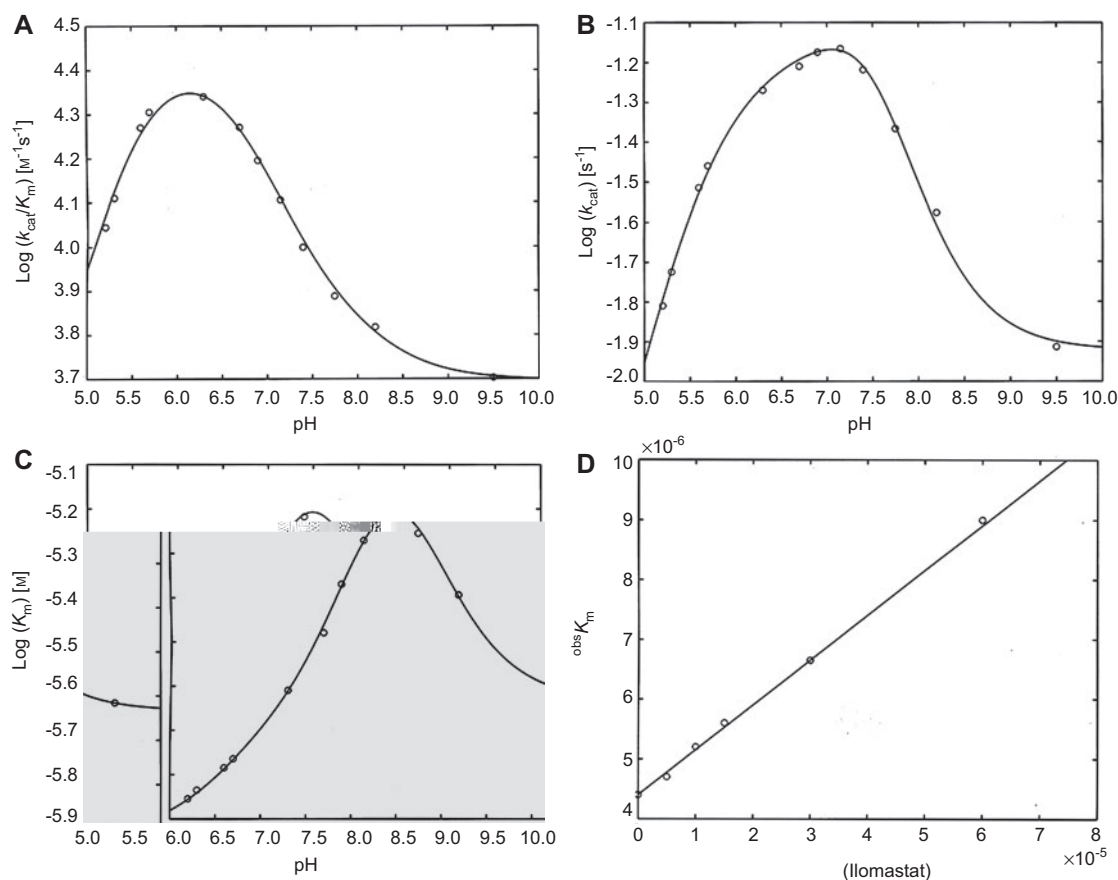

Figure 2 pH dependence of catalytic parameters for Zmp1 at 37°C against a synthetic fluorogenic substrate.
(A) pH dependence of k_{cat}/K_m. Continuous line represents the non-linear least squares fitting of data using Eq. (4a) with parameters reported in Table 2. (B) pH dependence of k_{cat}. Continuous line represents the nonlinear least squares fitting of data using Eq. (4b) with parameters reported in Table 2. (C) pH dependence of K_m. Continuous line represents the non-linear least squares fitting of data using Eq. (4c) with parameters reported in Table 2. (D) Ilomastat concentration dependence of substrate affinity constant K_m for Zmp1 at 37°C. Values of $^{obs}K_m$ have been obtained by Lineweaver-Burk plot of omni-MMPs fluorogenic peptide cleavage in the presence of Zmp1 (0.4 nM) in absence and presence of different Ilomastat concentrations (namely 5, 10, 15, 30, and 60 μM). The continuous line is the nonlinear least squares fitting of data according to Eq. (5), from which a value of ^0K_m=4.4(±0.6)×10⁻⁶ M and a value of K_I=5.9(±0.7)×10⁻⁵ are obtained.

Table 2 Catalytic parameters for the different protonated species of Zmp1 toward the synthetic fluorogenic substrate and pK_a values for the protonating groups in the free enzyme (pK_U) and of the substrate-bound enzyme (pK_L).

	k_{cat}/K_m ($\mathrm{M^{-1}\ s^{-1}}$)	k_{cat} ($\mathrm{s^{-1}}$)	K_m (M)
0-Protonated	5.0 ($\pm$0.7)$\times10^3$	0.012$\pm$0.004	2.4 ($\pm$0.4)$\times10^{-6}$
1-Protonated	7.1 ($\pm$0.9)$\times10^3$	0.131$\pm$0.029	1.9 ($\pm$0.3)$\times10^{-5}$
2-Protonated	3.0 ($\pm$0.5)$\times10^4$	0.065$\pm$0.017	2.2 ($\pm$0.5)$\times10^{-6}$
3-Protonated	9.5 ($\pm$1.6)$\times10^2$	0.008$\pm$0.001	8.4 ($\pm$1.6)$\times10^{-6}$
pK_{U1}	8.17$\pm$0.16		
pK_{U2}	6.73$\pm$0.17		
pK_{U3}	5.43$\pm$0.19		
pK_{L1}	7.22$\pm$0.18		
pK_{L2}	7.72$\pm$0.17		
pK_{L3}	5.69$\pm$0.18		

Eq. (5) (see Materials and methods) allows to determine the K_I [=5.9($\pm$0.7)$\times10^{-5}$ M], which is about 10^5-fold higher than that observed for matrix metallopeptidases (Galardy et al., 1994), reflecting a very low affinity of Ilomastat for Zmp1. This result indicates that Ilomastat is a very weak inhibitor for Zmp1, confirming the known difference between gluzincins and metzincins, as indeed it turns out to be evident also from the crystallographic structure, where the catalytic site results different from that of other metallopeptidases (Ferraris et al., 2011).

Zmp1 hydrolyzes a variety of bioactive peptides

To possibly identify the native substrate(s) of Zmp1, we carried out an extensive screening of a microarray-based peptide library. The library consists of 1989 octameric peptides derived from annotated cleavage sites of peptidases or random sequences and 1536 pentadecameric random peptide sequences. Peptides are C-terminally tagged with a phosphorylated tyrosine for detection. Peptide cleavage was quantified by incubation with antiphosphotyrosine and fluorescent secondary antibody labeling and following fluorescence measurement. Fluorescence intensity of 51 out of 3525 peptide spots was decreased by more than 90% as compared with the bovine serum albumin control. The 51 substrates were categorized into three groups (Table S1): (1) neuropeptides/substrates of NEP or endothelin-converting enzyme 1 (ECE-1); (2) coagulation factors; (3) others. Interestingly, only short peptides (octameric) were represented among the top substrates. The relative frequency of each amino acid in the efficiently cleaved peptides was calculated by dividing the number of times this specific amino acid is represented in the screened substrates over the number of times that the amino acid is represented in the whole peptide microarray. This statistical analysis provides information about the amino acid preferences in the substrates, although it does not allow prediction of actual cleavage sites. The most common motif among the top substrates was the sequence SPFR, which is present in the carboxy terminal part of the peptide hormone bradykinin. In particular, the statistical analysis showed an overrepresentation of arginine, phenylalanine, isoleucine, leucine, and valine in the top substrate sequences, whereas acidic amino acids such as aspartic or glutamic acid were underrepresented, and no cysteine or tryptophan were present in any of the 51 top substrates.

Zmp1 cleavage motif

Several cleavage motifs can be described from the MALDI-TOF cleavage analysis of the investigated peptides (Figure 3A). The phenylalanine was the most represented residue at P1′ position (Figure 3B), although isoleucine and leucine were also abundant at this position. Proline was frequently found in the P3 site, although other positions near the cleavage site showed little preference. We conclude that PxxF is a preferred cleavage motif of Zmp1 and phenylalanine occupies P1′ position.

Identification of substrate cleavage sites

First, we characterized the cleavage pattern of several neuropeptides identified in the peptide array (i.e., bradykinin, apelin-13, neurotensin, neuropeptide FF), including some NEP or ECE-1 substrates [i.e., substance P, dynorphin A (1–13), and
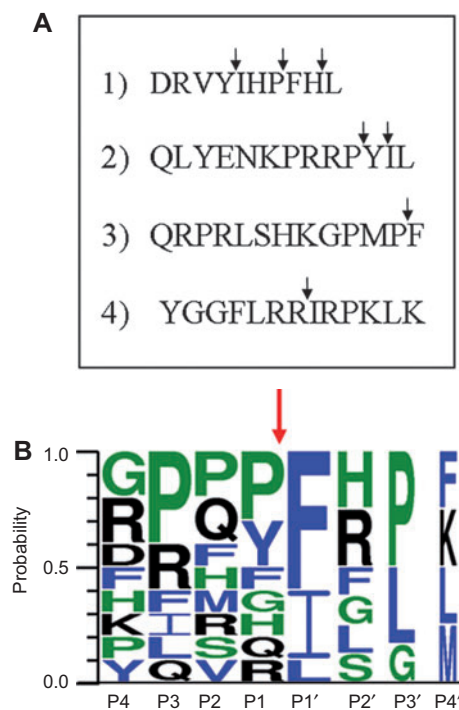
Figure 3 Hydrolysis of hormone peptides by Zmp1. (A) Cleavage sites detected in the Zmp1 hydrolyzed fluorogenic peptides: 1, angiotensin I; 2, neurotensin; 3, apelin-13; 4, dynorphin A (1–13). Neuropeptide FF cleavage pattern was not studied because of poor detection signals in the MALDI-TOF analysis. (B) Amino acid preferences at various position of Zmp1 substrates calculated on the basis of the cleavage pattern of the studied hormone peptides. Size of amino acid letter is proportional to their occurrence in the recognition/cleavage motif. Cleavage site (marked with red arrow) is localized between position P1 and P1′ (drawn using Weblogo 3.0).

angiotensin I], and the reaction by-products were analyzed by MALDI-TOF; to guarantee specific cleavage, a high substrate/enzyme ratio was used (1000:1). Two cleavage sites were detected in bradykinin (Figure 4A), i.e., between Pro[7]-Phe[8] and Gly[4]-Phe[5], confirming the results obtained with the extended bradykinin, which is generated by the proteolytic cleavage of the precursor kininogen-1 by the enzyme kallikrein (Kaplan et al., 2002). As a matter of fact, in rat, mouse, bovine, and human, the SPFR motif of kininogen-1 is conserved, but it is followed by a different carboxy terminal amino acid. Four zinc

metallopeptidases are mainly responsible for the metabolism of bradykinin, namely angiotensin-converting enzyme (ACE), NEP, aminopeptidase P, and carboxypeptidases M and N (Moreau et al., 2005). Both cleavages resulted in two respective fragments that were detected by MALDI-TOF (Figure 4B and C). We determined three cleavage sites in substance P: between Gln[6]-Phe[7], Phe[7]-Phe[8], and Gly[9]-Leu[10] (Figure 4D; Figure S2). Interestingly, all the cleavage sites of bradykinin and substance P have a hydrophobic amino acid in the P1′ site, mainly phenylalanine, which is typical of NEP, ECE-1, and thermolysin;
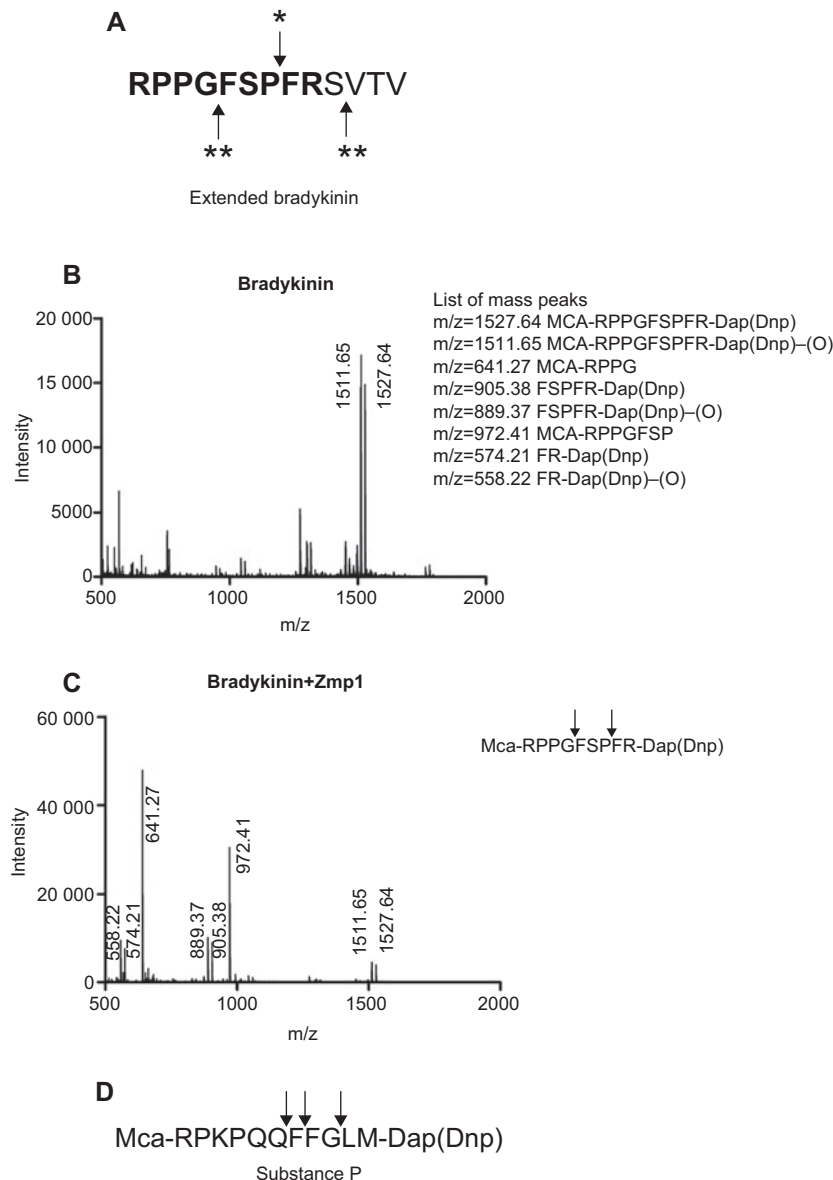

Figure 4 Cleavage sites of bradykinin and substance P by Zmp1.
(A) Determination of fragments of the 'extended' bradykinin (bradykinin sequence in bold) by Zmp1 through LC-MS analysis. Three different cleavage sites were detected in bradykinin. Primary site of hydrolysis is shown by the arrow with one asterisk, and secondary sites are shown by the arrows with two asterisks. (B) MALDI-TOF spectrum of fluorogenic bradykinin. (C) MALDI-TOF spectrum of Zmp1 hydrolyzed fluorogenic bradykinin. The C-terminal fragments showed an additional mass peak (Δ16 Da), due to a loss of oxygen (as described recently for nitro-phenyl-derivatives; see Petersson et al., 2001). (D) Cleavage sites of fluorogenic substance P by Zmp1. The arrows above the amino acid sequence of substance P indicate the cleavage sites.

further, this observation is in agreement with the overrepresentation of this amino acid in the top substrates as compared with the total peptide library. Specific sites of cleavage within the other neuropeptides, such as angiotensin I (Figure S3), apelin-13 (Figure S4), dynorphin A (1–13) (Figure S5), and neurotensin (Figure S6) are summarized in Figure 3A.

Further, we synthesized a peptide fragment of mouse kininogen with the sequence RPPGFSPFRSVTV to map the cleavage site (bradykinin sequence in bold). The peptide was incubated with Zmp1 for 60 and 120 min, respectively, and products were analyzed by LC-MS. Cleavage sites were determined by calculating the molecular weight of putative products (data not shown). Primary cleavage occurred between Pro[7] and Phe[8] (Figure 4A, arrow with one star). This cleavage site lies within the bradykinin sequence and results in the inactivation of bradykinin rather than releasing bradykinin from its precursor. This peptide bond is also targeted by ACE, the main enzyme responsible for the metabolism of bradykinin (Blais et al., 2000). Further cleavages were detected after longer incubation of the peptide with Zmp1, e.g., between Gly[4]-Phe[5] and Ser[10]-Val[11] (Figure 4A, arrows with two stars).

Kinetic analysis of neuropeptides cleavage

Zmp1 hydrolysis of the neuropeptides was further studied by the determination of kinetic constants K_m and k_{cat}. As the kinetic course of peptide cleavage by Zmp1 was affected by product inhibition and/or cleavage of multiple peptide bonds, initial velocities were exploited for calculating the kinetic parameters of the most susceptible peptide bond within a given peptide. Results are summarized in Table 3 as best fit values with associated standard errors from nonlinear regression of the Michaelis-Menten equation fitted to data. The kinetic parameters for angiotensin I and neurotensin could not be calculated because even the initial velocity was strongly affected by the concurrent multiple cleavage and multiple product inhibition. Figure 5A shows, as an example, the double reciprocal Lineweaver-Burk plot for substance P, apelin-13, and bradykinin; it clearly emerges that substance P and apelin-13 are the best substrates among those investigated.

pH dependence of substance P and apelin-13 hydrolysis

In several studies, ECE-1 was found to cleave neuropeptides inside acidified endosomes (i.e., at pH≈5.5) (Padilla et

Table 3 Kinetic parameters for the cleavage of the most susceptible peptide bond in five peptides substrates of Zmp1.

Substrate	k_{cat} (s^{-1})	K_m (µM)	k_{cat}/K_m (M^{-1} s^{-1})
Apelin	1.54±0.08	1.09±0.23	1.41±0.31×10^6
Substance P	4.78±0.71	3.92±1.37	1.22±0.46×10^6
Bradykinin	2.76±0.42	7.99±1.45	3.46±0.67×10^5
Dynorphin A	2.25±0.22	5.72±1.22	3.93±0.92×10^5
Neuropeptide FF	1.07±0.16	3.02±1.15	3.56±1.45×10^5

Values of k_{cat} and K_m, determined by non-linear regression from a fit of the Michaelis-Menten equation to primary data, are shown together with the standard errors from regression.
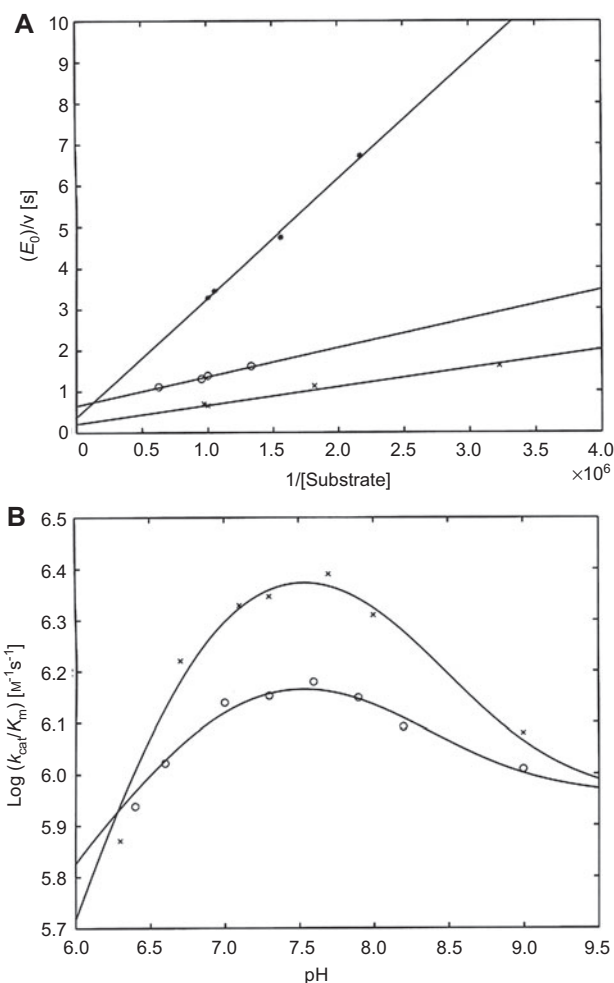

Figure 5 Kinetic analysis of Zmp1 hydrolysis of apelin-13, substance P, and bradykinin.
(A) Double-reciprocal Lineweaver-Burk plot of the enzymatic processing by Zmp1 of apelin-13 (o), substance P (x), and bradykinin (*) at 37°C and pH 7.3. Solid lines represent the non-linear least squares fitting of data according to Eq. (2). (B) pH dependence of the rate of cleavage (k_{cat}/K_m) of apelin-13 (o) and substance P (x) by Zmp1 at 37°C. Continuous lines represent the nonlinear least squares fitting of data according to Eq. (4a).

al., 2007; Roosterman et al., 2007). We determined the pH dependence of Zmp1 activity for additional substrates, i.e., apelin-13 and substance P to see the pH preference for these substrates. Zmp1 cleaved the two neuropeptides preferentially in the pH range between 6.5 and 8.0 rather than at more acidic pH values, as observed for the fluorogenic substrate (Figure 2 for the pH profile of the fluorogenic substrate, Figure 5B for that of substance P and apelin-13). Data obtained from the pH-dependence of apelin-13 and substance P degradation by Zmp1 are reported in Table 4.

Screening for macromolecular substrates (longer than 40 amino acids)

Using an *in vitro* proteolysis assay we have investigated the enzymatic action of Zmp1 on four of the substrates reported

Table 4   Values of k_{cat}/K_m (M^{-1} s^{-1}) for the different protonated species of Zmp1 toward apelin-13 and substance P and pK_a for the protonating groups in the free enzyme (pK_U).

	Apelin-13	Substance P
0-Protonated	9.0 (±1.6)×10^5	8.8 (±1.6)×10^5
1-Protonated	1.7 (±0.4)×10^6	3.1 (±0.7)×10^6
2-Protonated	6.5 (±1.1)×10^5	1.6 (±0.4)×10^5
3-Protonated	1.0 (±0.8)×10^4	1.0 (±0.7)×10^5
pK_{U1}	8.17± 0.16	
pK_{U2}	6.73±0.17	
pK_{U3}	5.43±0.19	

on the top substrates list of the peptide array: β-amyloid, α-fibrinogen chain, insulin, and denatured collagen. We have further tested Zmp1 proteolytic activity on caspase 1, the IL-1β activating enzyme. However, even prolonged exposition to Zmp1 (up to 24 h) did not lead to any appreciable cleavage of these potential substrates (data not shown). In contrast, a control incubation with trypsin led to complete digestion of the α-, β-, and γ-fibrinogen chains already after 1 h of incubation.

Discussion

Zinc metallopeptidases represent promising pharmacological targets and potential candidates for vaccine development (Miyoshi and Shinoda, 2000; Aureli et al., 2008; Lopez-Otin and Bond, 2008; Baillie et al., 2010). We have investigated the wt and the inactive mutants (H493A and E494A) of the metallopeptidase Zmp1, which is an important virulence factor of Mtb (Master et al., 2008).

Zmp1 belongs to the M13 family (MEROPS database: http://merops.sanger.ac.uk/), such as NEP and ECE-1, whose enzymatic action is restricted to peptides with a strong preference for cleaving the amino terminal bond of hydrophobic residues (Bland et al., 2008). This preference for peptides is also confirmed by the recently solved X-ray crystallographic structure of Zmp1, which reveals that the active site is located at the bottom of a hydrophobic channel, likely impairing the access of large macromolecular substrates in the proximity of the reaction centre (Ferraris et al., 2011).

To better characterize the specificity of Zmp1 a peptide microarray library was used (including octameric and pentadecameric peptides); in particular, octameric peptides were enzymatically cleaved with the highest efficiency. Further, a statistical analysis over the whole peptide array indicate a marked tendency of Zmp1 to cleave bonds where hydrophobic amino acids are located at the P1′ position, similarly to NEP and ECE-1. In addition, as shown by the *in vitro* cleavage assay, sequences identified by the peptide array could not be cleaved when they were flanked by the whole protein sequences in a context of a structurally complex molecule (e.g., fibrinogen, β-amyloid).

Among the hits screened, several neuropeptides have been identified [i.e., substance P, neurotensin, bradykinin, apelin-13, angiotensin I, neuropeptide FF, and dynorphin A (1–13)]. With respect to these, it is interesting to remark that a member of M13 family (ECE-1) localizes into the luminal side of endosomal membrane where it degrades internalized neuropeptides (e.g., substance P, apelin-13) (El Messari et al., 2004; Roosterman et al., 2007; Cottrell et al., 2009), suggesting their possible biological relevance as substrates of this type of enzymes. As a matter of fact, besides the classical involvement of neuropeptides in neurotransmission and vasal smooth muscle cells constriction, at least for some of them, a novel role in the modulation of immune responses has been envisaged (Skidgel et al., 1984; Johnson et al., 1999; Marriott and Bost, 2001; Yaraee et al., 2007), affecting proinflammatory cytokine and chemokine activation (in the case of apelin-13) and macrophage activation (in the case of the substance P) in the early phases of immune responses to *Salmonella* infection (Kincy-Cain and Bost, 1996; O'Connor et al., 2004; Leeper et al., 2009).

A comparison between the degradation profile of these substrates by Zmp1, NEP, and ECE-1 highlights overlapping specificities in terms of cleavage sites (i.e., for bradykinin, substance P, and dynorphin A) with minor differences (i.e., secondary cleavage sites in angiotensin I and neurotensin) (Matsas et al., 1984; Johnson et al., 1999). However, a significant quantitative difference in terms of catalytic efficiency with respect to ECE-1 is observed with k_{cat}/K_m ratios, which in Zmp1 are 100- and 5-fold higher for substance P and bradykinin, respectively (Johnson et al., 1999). On the whole, apelin-13 turns out to be an excellent substrate for Zmp1, being efficiently cleaved with the highest specificity constant (i.e., k_{cat}/K_m) among all tested peptides, a feature mostly related to the binding specificity rather than the cleavage efficiency.

Although we cannot state at this stage whether these neuropeptides represent the Zmp1 substrate *in vivo*, pH scanning of Zmp1 proteolytic activity toward all investigated peptides indicates that Zmp1 can modulate its activity through the dynamical pH changes that occur in the maturating phagosome. In this respect, it is noteworthy that degradation of neuropeptides by ECE-1 in endosomes under acidic conditions (i.e., pH 5.5) is documented (Fahnoe et al., 2000) and it is associated to intracellular signaling and receptor turnover (El Messari et al., 2004; Roostermann et al., 2007; Cottrell et al., 2009); analogously, we found that Zmp1 optimum activity toward the synthetic substrate is at pH 6.3 (Figure 2A), a value corresponding to that of the early endosome (Pethe et al., 2004). Therefore, it might be speculated that, similarly to ECE-1, Zmp1 operates within the phagosome, arresting its maturation (Master et al., 2008; Johansen et al., 2011). As a matter of fact, at the acid pH of the maturating phagosome (i.e., pH 6.3), the substrate affinity of Zmp1 is fairly high (i.e., 2 μM), suggesting a conformation of the active site particularly suitable to interact with substrates under quite acidic pH conditions. In the case of neuropeptides, such as apelin-13 and substance P, the optimum pH is somewhat higher than that observed for the synthetic substrate, although pK_a values for the pH dependence of k_{cat}/K_m are fully comparable. This strongly supports the idea that these pK_a values refer only to the protonation of Zmp1 residues with no contribution from residues of the substrate(s). Therefore, as the whole enzymatic mechanism of Zmp1 seems to be modulated by the protonation of three classes of residues

(characterized by pK_{a1}, pK_{a2}, and pK_{a3}, respectively), the different pH profiles between these substrates can be simply explained by the involvement of different protonated species (the 2-protonated for the synthetic substrate and the 1-protonated for neuropeptides). This feature is clearly reflecting a relevant difference between the two classes of substrates in their ionic interactions with the enzyme.

These investigations demonstrate the importance of Zmp1 for mycobacteria host interaction and highlight its potential as a pharmacological target. Two major conclusions can be drawn: Zmp1 preferentially cleaves small peptides, among which neuropeptides appear particularly interesting; Zmp1 adapts its activity to different microenvironmental conditions. The present biochemical characterization of the enzymatic properties of Zmp1 can be merged with the structural information on Zmp1 (Ferraris et al., 2011), allowing a structural-functional correlation, which will be of the utmost importance for a rational drug design.

Materials and methods

Molecular cloning and protein expression

Mtb *Zmp1* gene was subcloned into pET100/D-TOPO® vector (Invitrogen) using a PCR-amplified product from pMV361-Zmp1 vector, carrying *Zmp1* gene, as previously reported (Master et al., 2008).

For all constructs, 1-L overnight culture of *E. coli* BL21 (Invitrogen) in L-broth medium (induced at OD_{600}=0.8 with 0.5 mM IPTG and grown at 18°C) was centrifuged at 5000 *g* for 20 min, followed by washing with PBS and additional centrifugation at 5000 *g* for 20 min. Cells were then lysed by three French press cycles (Thermo Electron) at $1.4×10^8$ Pa in the presence of peptidase inhibitors, followed by ultracentrifugation at 30 000 *g* for 60 min. Supernatants were loaded on HisTrap™ HP column (GE Healthcare) equilibrated with buffer containing 20 mM NaH_2PO_4, pH 7.4, 0.5 M NaCl. Proteins were eluted with a concentration gradient of imidazole. Both Zmp1 and GST-Zmp1 were eluted at 250 mM imidazole (protein concentration was 0.5–1 mg/ml). After overnight dialysis against PBS, Zmp1 wt was further purified by ion exchange using a Q Column (GE Healthcare). GST-Zmp1 purification was performed using glutathione-sepharose beads (Glutathione Sepharose 4B; GE Healthcare). Proteins were dialyzed against PBS, and finally, glycerol at a final concentration of 10% was added to store them in aliquots at -20°C. Proteins were analyzed by 12.5% SDS-gel and subsequent Coomassie stain or Western blot against HA. All chemicals used were from Acros, Applichem, Fluka or Sigma-Aldrich. For detection of recombinant Zmp1 the following antibodies are used: mouse anti-HA (Roche) and goat anti-mouse-HRP (Molecular Probes).

CD experiments

CD spectra for the validation of the correct folding of the protein were recorded on a Jasco J-710 spectropolarimeter equipped with a thermostated cell holder and connected to a data station for signal averaging and processing. All spectra were averages of four scans and were recorded using quartz cells of 2-mm path length. Zmp1 was dissolved in CD buffer (20 mM Tris-HCl, 1 mM $CaCl_2$, 100 mM NaCl) at about 2 μM concentration. The α-helix content of Zmp1 was calculated from the molar ellipticity of circular dichroic spectrum at 222 nm according to the following equation

$$\% \text{ α-helix} = (-[\theta]_{222\,nm} + 3000)/39\,000 \tag{1}$$

where $[\theta]_{222\,nm}$ is the molar ellipticity at 222 nm, as previously described (Morrow et al., 2000).

Kinetic analysis and pH dependence of Zmp1 catalysis

Internally quenched fluorogenic substrates with 7-methoxycoumarin (MCA) as fluorophore and 2,4-dinitrophenol (DNP) as quencher were either a synthetic fluorogenic substrate, displaying the following sequence:

[(MCA-yl)acetyl]-Pro-Leu-Gly-Leu-DNP[*N*-3-(2,4-dinitrophenyl)-L-2,3-diaminopropionyl]-Ala-Arg-NH$_2$)

or neuropeptides from EMC microcollections (Tübingen, Germany). Neurotensin was synthesized with glutamine as N-terminal amino acid instead of pyroglutamic acid for ease of synthesis. The substrate peptides were prepared as stock solutions in 100% dimethyl sulfoxide (DMSO) at a final concentration of 1.0 mM and further diluted into the universal buffer (25 mM bis-Tris-HCl, 25 mM Tris-HCl, 100 mM NaCl, and 10 mM $CaCl_2$ prepared at 25°C) to maintain an unaltered composition at different pH values over the range investigated, keeping the DMSO concentration constant at 1% (v/v) for all dilutions. Substrate hydrolysis was measured fluorometrically with an Eclypse fluorimeter (Varian) or with a Flx800 spectrofluorometer (BIOTEK) equipped with KC Junior Software (BIOTEK) (λ_{exc}=327 nm, λ_{em}=393 nm); reactions were started by adding Zmp1 (at a final concentration of 10 nM) to a solution containing different substrates concentrations, spanning between 0.3 μM and 5 μM. For the pH dependence, Zmp1 was incubated in the universal buffer between pH 5.2 and 9.5 for 5 min at 37°C, then substrate was added, and fluorescence signal was followed. Background fluorescence of all buffers was similar. The initial velocities were measured at 37°C within a time interval during which the rate was constant and <10% of the substrate has been degraded. It ensured a steady-state condition, and it was a prerequisite for the subsequent analysis step, which was based on the observation of an inverse linear correlation between velocity and substrate concentration according to Lineweaver-Burk equation [Eq. (2)] and Eadie-Hofstee linear regression [Eq. (3)]

$$\frac{E_0}{v} = \frac{K_m}{k_{cat}} \cdot \frac{1}{[S]} + \frac{1}{k_{cat}} \tag{2}$$

$$\frac{v}{S} = \frac{V_{MAX}}{K_m} - \frac{v}{K_m} + \frac{K_m + S}{K_m S}\varepsilon \tag{3}$$

where E_0 is the total enzyme concentration, v is the actual rate (expressed as mol/s), K_m is the Michaelis-Menten equilibrium constant (expressed as mol), k_{cat} is the rate-limiting step kinetic constant (expressed as s^{-1}), $[S]$ is the substrate concentration, and V_{MAX} is the ratio between E_0 and v. Linear regression plots were constructed from the velocity data, and the catalytic parameters k_{cat} and K_m were extracted. The pH dependence of the catalytic parameters has been fitted according to the following equations

$$^{obs}k_{cat}/K_m = \frac{\sum_{i=0}^{i=n} {}^{i}k_{cat}/K_m \cdot \prod_{r=0}^{r=i} {}^{r}K_{ua} \cdot [H^+]^r}{\sum_{i=0}^{i=n}\prod_{r=0}^{r=i} {}^{r}K_{ua} \cdot [H^+]^r} \tag{4a}$$

$$^{obs}k_{cat} = \frac{\sum_{i=0}^{i=n} {}^{i}k_{cat} \cdot \prod_{r=0}^{r=i} {}^{r}K_{La} \cdot [H^+]^r}{\sum_{i=0}^{i=n}\prod_{r=0}^{r=i} {}^{r}K_{La} \cdot [H^+]^r} \tag{4b}$$

$$^{\mathrm{obs}}K_{\mathrm{m}} = {}^{0}K_{\mathrm{m}} \cdot \frac{\sum\limits_{i=0}^{i=n}\prod\limits_{r=0}^{r=i} {}^{r}K_{\mathrm{ua}} \cdot \left[H^{+}\right]^{r}}{\sum\limits_{i=0}^{i=n}\prod\limits_{r=0}^{r=i} {}^{r}K_{\mathrm{La}} \cdot \left[H^{+}\right]^{r}} \tag{4c}$$

where $^{\mathrm{obs}}k_{\mathrm{cat}}/K_{\mathrm{m}}$, $^{\mathrm{obs}}k_{\mathrm{cat}}$, and $^{\mathrm{obs}}K_{\mathrm{m}}$ are the observed parameters as a function of pH; $^{i}k_{\mathrm{cat}}/K_{\mathrm{m}}$, $^{i}k_{\mathrm{cat}}$, and $^{i}K_{\mathrm{m}}$ are the parameters for the ith-protonated forms; $^{i}K_{\mathrm{ua}}$ are the ith protonation constants for the free enzyme E; and $^{i}K_{\mathrm{La}}$ are the ith protonation constant(s) for the substrate-bound enzyme ES when it is involved in the cleavage event at the rate-limiting step. The global fitting procedure, simultaneously using Eqs. (4a)–(4c) to describe the pH dependence of all three catalytic parameters of Zmp1 (i.e., $k_{\mathrm{cat}}/K_{\mathrm{m}}$, k_{cat}, and K_{m}), allows to determine the pK_{a} of protonating groups, which modulate the enzymatic activity of Zmp1.

Inhibition assay

For inhibition experiments, Zmp1 (10 nM) was preincubated with EDTA, phosphoramidon, and 1,10-phenanthroline (Sigma) in the universal buffer (see above) at room temperature before addition of the synthetic fluorogenic substrate. Fluorescence was measured after 5 min of incubation with the fluorogenic substrate (5 μM) at 37°C. In the case of Ilomastat (British Biotech Pharmaceutical, Cowley, Oxford, UK), the inhibition constant K_{I} was measured obtaining the various K_{m} from the substrate concentration dependence at various inhibitor concentration, using Eqs. (2) and (3) and then plotting data of K_{m} as a function of inhibitor concentration, as from the following equation

$$K_{\mathrm{m}} = {}^{0}K_{\mathrm{m}} \cdot \left(1 + \frac{[I]}{K_{\mathrm{I}}}\right) \tag{5}$$

where K_{m} is the Michaelis constant at different inhibitor concentrations, $^{0}K_{\mathrm{m}}$ is the Michaelis constant in the absence of the inhibitor, $[I]$ is the inhibitor concentration, and K_{I} is the inhibition constant.

Peptide array

Peptide array was performed at JPT Berlin using a commercially available microarray (batch 1562, both for peptidase incubation and control incubation in triplicates; JPT Peptide Technologies GmbH, Berlin, Germany). The library consists of 1989 octameric peptides derived from annotated cleavage sites of peptidases or random sequences and 1536 pentadecameric random peptide sequences. Peptides contain a C-terminal phosphorylated tyrosine for detection with an antiphosphotyrosine antibody. The peptide microarray was incubated with 10 μg/ml Zmp1 (total reaction volume 400 μl) for 4 h at 37°C, using a microarray sandwich-like construction. As a control sample, an additional incubation was carried out in the absence of the target peptidase, which was followed by washing steps with 50 mM TBS buffer, pH 7.2, and ddH$_2$O. Subsequent drying with a microarray centrifuge was performed. Microarrays were first incubated with anti-pTyr-antibody (for about 45 min) and then for 30 min with Dylight 649-labeled antimouse-antibody. For detection, a Tecan HS4800 microarray processing station was used. Total incubation time was 45 min for anti-pTyr-100-antibody and 30 min for antimouse-antibody, followed by washing steps with 50 mM TBS, pH 7.2, and SSC buffer, pH 7.0 (JPT). Finally, the microarray plates were dried using a nitrogen stream. Analysis was performed with high-resolution fluorescence scanner (Axon Genepix 4200 AL Scanner), and Spot-recognition software Genepix 6.0 and Microsoft Excel were used for data analysis. A reduction by more than 90% of signal intensity was considered as effective cleavage.

Cleavage site determination by MALDI-TOF

Peptide cleavage assay was performed as following: 100 μM neuropeptides were incubated with or without Zmp1 (20 nM) for 5 min at 37°C in a total volume of 200 μl. Then, 1 μl of a 1:100 dilution with MALDI Matrix solution (consisting of 60% acetonitrile, 0.1% trifluoroacetic acid in ddH$_2$O, and 4 mg/ml α-cyano-4-hydroxy cinnamic acid) was spotted on the MALDI plate. After evaporation of solutes, MALDI spectra were recorded with a 4800 plus MALDI TOF/TOF Analyzer (Applied Biosystems, Foster City, CA, USA). MALDI was equipped

Bland, N.D., Pinney, J.W., Thomas, J.E., Turner, A.J., and Isaac, R.E. (2008). Bioinformatic analysis of the neprilysin (M13) family of peptidases reveals complex evolutionary and functional relationships. BMC Evol. Biol. *8*, 16.

Carson, J.A. and Turner, A.J. (2002). Beta-amyloid catabolism: roles for neprilysin (NEP) and other metallopeptidases? J. Neurochem. *81*, 1–8.

Cole, S.T., Eiglmeier, K., Parkhill, J., James, K.D., Thomson, N.R., Wheeler, P.R., Honore, N., Garnier, T., Churcher, C., Harris, D., et al. (2001). Massive gene decay in the leprosy bacillus. Nature *409*, 1007–1011.

Cottrell, G.S., Padilla, B.E., Amadesi, S., Poole, D.P., Murphy, J.E., Hardt, M., Roosterman, D., Steinhoff, M., and Bunnett, N.W. (2009). Endosomal endothelin-converting enzyme-1: a regulator of beta-arrestin-dependent ERK signaling. J. Biol. Chem. *284*, 22411–22425.

El Messari, S., Iturrioz, X., Fassot, C., De Mota, N., Roesch, D., and Llorens-Cortes, C. (2004). Functional dissociation of apelin receptor signaling and endocytosis: implications for the effects of apelin on arterial blood pressure. J. Neurochem. *90*, 1290–1301.

Fahnoe, D.C., Knapp, J., Johnson, G.D., and Ahn, K. (2000). Inhibitor potencies and substrate preference for endothelin-converting enzyme-1 are dramatically affected by pH. J. Cardiovasc. Pharmacol. *36*, S22–S25.

Fasciglione, G.F., Marini, S., D'Alessio, S., Politi, V., and Coletta, M. (2000). pH- and temperature-dependence of functional modulation in metalloproteinases. A comparison between neutrophil collagenase and gelatinases A and B. Biophys. J. *79*, 2138–2149.

Ferraris, D.M., Sbardella, D., Petrera, A., Marini, S., Amstutz, B., Coletta, M., Sander, P., and Rizzi, M. (2011). Crystal structure of *Mycobacterium tuberculosis* zinc-dependent metalloprotease-1 (Zmp1), a metalloprotease involved in pathogenicity. J. Biol. Chem. *286*, 32475–32482.

Galardy, R.E., Cassabonne, M.E., Giese, C., Gilbert, J.H., Lapierre, F., Lopez, H., Schaefer, M.E., Stack, R., Sullivan, M., Summers, B., et al. (1994). Low molecular weight inhibitors in corneal ulceration. Ann. NY Acad. Sci. *732*, 315–323.

Johansen, P., Fettelschoss, A., Amstutz, B., Selchow, P., Waeckerle-Men, Y., Keller, P., Deretic, V., Held, L., Kundig, T.M., Bottger, E.C., et al. (2011). Relief from Zmp1-mediated arrest of phagosome maturation is associated with facilitated presentation and enhanced immunogenicity of mycobacterial antigens. Clin. Vaccine Immunol. *18*, 907–913.

Johnson, G.D., Stevenson, T., and Ahn, K. (1999). Hydrolysis of peptide hormones by endothelin-converting enzyme-1. A comparison with neprilysin. J. Biol. Chem. *274*, 4053–4058.

Kaplan, A.P., Joseph, K., and Silverberg, M. (2002). Pathways for bradykinin formation and inflammatory disease. J. Allergy Clin. Immunol. *109*, 195–209.

Kincy-Cain, T. and Bost, K.L. (1996). Increased susceptibility of mice to Salmonella infection following in vivo treatment with the substance P antagonist, spantide II. J. Immunol. *157*, 255–264.

Leeper, N.J., Tedesco, M.M., Kojima, Y., Schultz, G.M., Kundu, R.K., Ashley, E.A., Tsao, P.S., Dalman, R.L., and Quertermous, T. (2009). Apelin prevents aortic aneurysm formation by inhibiting macrophage inflammation. Am. J. Physiol. Heart Circ. Physiol. *296*, H1329–H1335.

Lopez-Otin, C. and Bond, J.S. (2008). Proteases: multifunctional enzymes in life and disease. J. Biol. Chem. *283*, 30433–30437.

Madani, R., Poirier, R., Wolfer, D.P., Welzl, H., Groscurth, P., Lipp, H.P., Lu, B., El Mouedden, M., Mercken, M., Nitsch, R.M., et al. (2006). Lack of neprilysin suffices to generate murine amyloid-like deposits in the brain and behavioral deficit in vivo. J. Neurosci. Res. *84*, 1871–1878.

Marriott, I. and Bost, K.L. (2001). Substance P receptor mediated macrophage responses. Adv. Exp. Med. Biol. *493*, 247–254.

Masjedi, M.R., Farnia, P., Sorooch, S., Pooramiri, M.V., Mansoori, S.D., Zarifi, A.Z., Akbarvelayati, A., and Hoffner, S. (2006). Extensively drug-resistant tuberculosis: 2 years of surveillance in Iran. Clin. Infect. Dis. *43*, 841–847.

Master, S.S., Rampini, S.K., Davis, A.S., Keller, C., Ehlers, S., Springer, B., Timmins, G.S., Sander, P., and Deretic, V. (2008). *Mycobacterium tuberculosis* prevents inflammasome activation. Cell Host Microbe *3*, 224–232.

Matsas, R., Kenny, A.J., and Turner, A.J. (1984). The metabolism of neuropeptides. The hydrolysis of peptides, including enkephalins, tachykinins and their analogues, by endopeptidase-24.11. Biochem. J. *223*, 433–440.

Miyoshi, S. and Shinoda, S. (2000). Microbial metalloproteases and pathogenesis. Microbes Infect. *2*, 91–98.

Moreau, M.E., Garbacki, N., Molinaro, G., Brown, N.J., Marceau, F., and Adam, A. (2005). The kallikrein-kinin system: current and future pharmacological targets. J. Pharmacol. Sci. *99*, 6–38.

Morrow, J.A., Segall, M.L., Lund-Katz, S., Phillips, M.C., Knapp, M., Rupp, B., and Weisgraber, K.H. (2000). Differences in stability among the human apolipoprotein E isoforms determined by the amino-terminal domain. Biochemistry *39*, 11657–11666.

Muttucumaru, D.G., Smith, D.A., McMinn, E.J., Reese, V., Coler, R.N., and Parish, T. (2011). *Mycobacterium tunerculosis* Rv0198c, a putative matrix metalloprotease, is involved in pathogenicity. Tuberculosis (Edinb) *91*, 111–116.

Nguyen, L. and Pieters, J. (2005). The Trojan horse: survival tactics of pathogenic mycobacteria in macrophages. Trends Cell Biol. *15*, 269–276.

O'Connor, T.M., O'Connell, J., O'Brien, D.I., Goode, T., Bredin, C.P., and Shanahan, F. (2004). The role of substance P in inflammatory disease. J. Cell Physiol.